Chapter 6

Power Electronic Solutions to Improve the Performance of Lundell Automotive Alternators

Ruben Ivankovic, Jérôme Cros, Mehdi Taghizadeh Kakhki,
Carlos A. Martins and Philippe Viarouge

Additional information is available at the end of the chapter

http://dx.doi.org/10.5772/46854

1. Introduction

Until in the early 1960s, automobiles used a DC generator called dynamo. The availability of affordable power diodes in the beginning of 1960s paved the way for the widespread use of three-phase claw-pole alternators (or Lundell alternators) for the generation of electric power in motor vehicles. After more than 50 years, this system is still the most economic choice in today's vehicles due to its low manufacturing cost. However, the efficiency and output power of the Lundell alternators are limited. This is a major drawback for its use in modern vehicles requiring an increase in electrical power. Many alternatives are being considered to replace the Lundell alternator such as the salient pole machines, however they require large investments in manufacturing infrastructure. In this context, this chapter focuses on the improvements of Lundell alternators that could represent the best solutions for the short term. First, we present the conventional automotive generating system, its performance and the limitation of modelling methods. We also discuss various solutions to increase the output power of Lundell alternators without any geometry modification. These include the use of reconfigurable windings and replacement of the diode rectifier by different electronic converters such as a synchronous rectifier or an interleaved PWM rectifier will be considered.

2. Generating system with a Lundell alternator

Today, the great majority of electrical generator systems installed on combustion powered vehicles are based on a three-phase wound-field synchronous machine. The conventional automotive generator has a claw pole rotor with a single excitation coil wound axially. It is often named "Lundell" alternator (Fig. 1). The excitation coil is surrounded by two solid iron pole pieces, or claw poles, and is fed via a pair of slip rings and two carbon brushes.

The stator is composed of a slotted laminated iron core and a three-phase overlapped winding, wye or delta connected. It is a wave-winding in most cases. Fig. 1 shows a dismantled Lundell alternator (Delcotron 22SI) and its main components. The number of rotor poles for passenger vehicles is generally fixed at 12 poles. The stator has often a single slot per pole and per phase (36 total slots). High power alternators for some applications like buses, trucks or other special vehicles have higher pole numbers (between 14 and 18). Increasing the number of poles reduces the inductance of the stator winding, and as a result, increases the short circuit current. Unfortunately the magnetic losses will also increase due to the higher electrical frequency. So the choice of pole number is actually based on a compromise between the magnetic losses and alternator power requirements. The alternator is coupled to the combustion motor through a belt. In passenger cars the maximum alternator speed (typically 8000 RPM) is about two times more than that of the engine crankshaft (a pulley ratio of 1:2). The Lundell alternator is generally characterized by its form factor (a relatively large diameter compared to its length) which facilitates thermal dissipation.

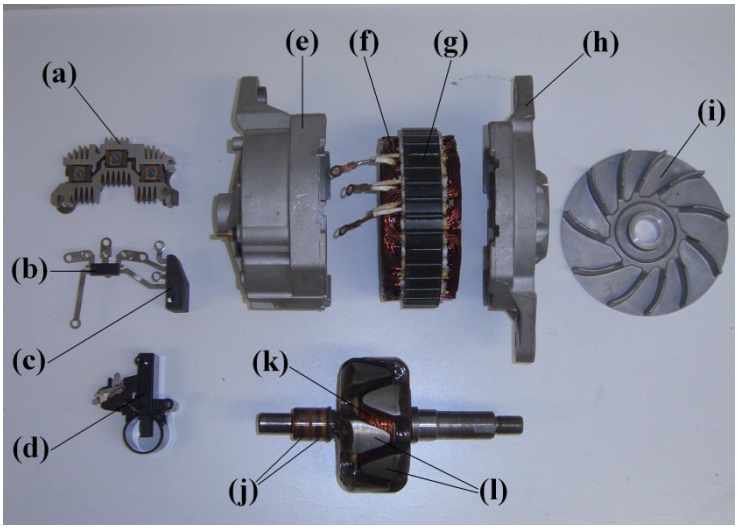

Figure 1. Dismantled alternator parts: (a) 6 diode full- bridge power rectifier, (b) excitation rectifier, (c) regulator, (d) brush assembly, (e) aluminum rear housing, (f) stator winding, (g) stator laminated core, (h) aluminum front housing, (i) aluminum fan, (j) slip rings, (k) excitation winding, (l) claw-shaped pole pieces.

2.1. Electrical circuit

Fig. 2 shows the simplified schema of a vehicle generation system. Usually six diodes in a full-bridge configuration are used to rectify the output current. The rectifier is divided in two sets of three diodes. The metal casing of the first set is typically pressed into a heat sink (or welded to the heat sink) for better thermal dissipation.

The output power is controlled by regulating the field current. The regulator maintains a constant output voltage on the battery despite the varying alternator speed and variable load conditions. This voltage depends highly on the ambient temperature and the chemical characteristics of the battery and necessitates a temperature compensation by the regulator. The regulator-excitation circuit is often supplied by an additional half- bridge rectifier instead of the battery (Exciter rectifier).

In the alternators with wye connected windings, two or more other auxiliary diodes are connected between the neutral point and the main rectifier output terminals. In this way it is possible to rectify the induced third harmonic voltage and increase the output current at high speeds.

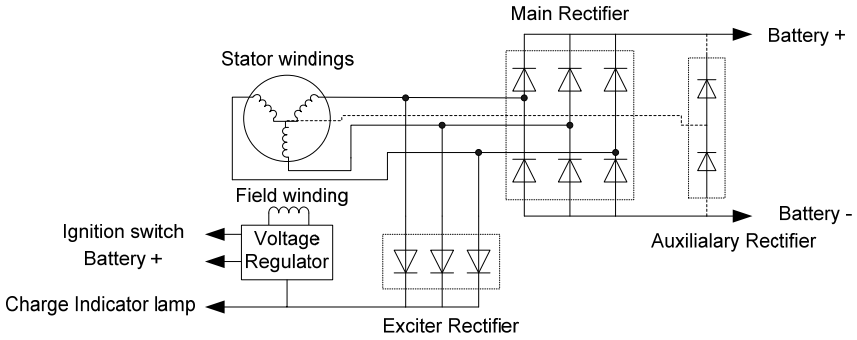

Figure 2. Simplified schema of conventional vehicle generating system with a Lundell alternator.

2.2. Alternator performance curves

Performance curves of an alternator are used to show its performance across the whole speed range. Fig. 3 shows the performance curves of a 100A commercial alternator obtained for a battery voltage of 14 V, an ambient temperature of 25° C, and for the maximum excitation current (near 6A).

The output current curve is characterized essentially by three operation points. The first one is the generation starting speed (Ω_{DG}) or 0-Ampere speed at which the alternator reaches its rated voltage without delivering power. The second one is the maximum output current at the highest speed, which corresponds approximately to the DC short-circuit current of the alternator (I_{SC}). Also, a special attention is paid to the output power requirement at engine idle speed (Ω_R) at which the alternator must deliver at least the power needed for long-term consumers. No output power is required below the idle speed. Another operating point often mentioned is the speed at rated current (Ω_N).

2.3. Alternator efficiency

Generally, Lundell alternators are characterized by low efficiency due to important mechanical, copper, and magnetic losses. The efficiency of the alternator varies widely

depending on load conditions, alternator speed and alternator size. As shown in fig. 3, the efficiency is only 53% at idle speed (losses: 675W) and about 42% at 6000 RPM (losses: 2100W). Larger and heavier alternators may be more efficient for the same speed and load conditions, however, this advantage can be compensated by the increase in fuel consumption due to the higher weight (0.1 L/100km fuel consumption for each additional 10 kg for a medium sized vehicle)(Beretta, 2008). Table 1 shows the distribution of losses in an alternator (Beretta, 2008) for two different speeds (full excitation field).

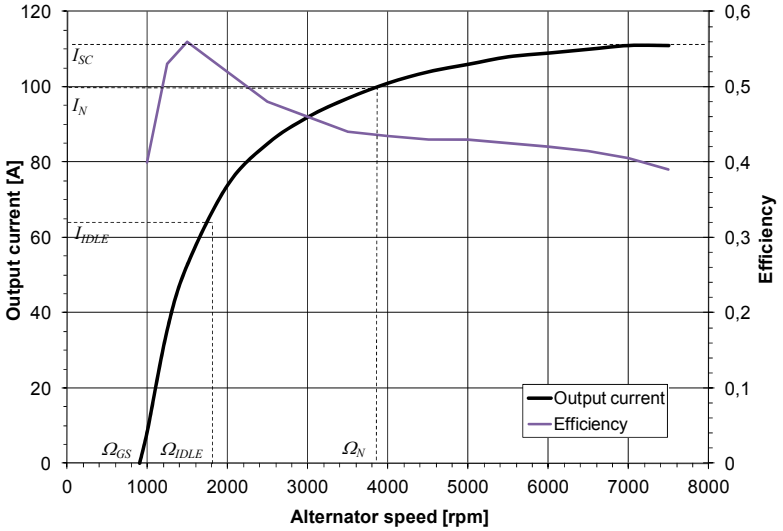

Figure 3. Characteristic of the output maximum current and efficiency as a function of speed for an alternator (Delcotron 22SI type12V-100A) at a battery voltage of 14V, ambient temperature of 25° C and maximum excitation current.

	1800 RPM	6000 RPM
Mechanical losses	2%	6%
Excitation losses (rotor)	7%	3%
Magnetic losses (stator)	21%	20%
Copper losses (stator)	49%	57%
power rectifier losses	21%	14%

Table 1. Distribution of losses in an alternator for two different speeds (full excitation field).

2.3.1. Mechanical losses

Mechanical losses are generated by brush and bearing friction and losses created by the claw pole rotor and fan (windage losses). The mechanical losses increase considerably at higher speeds (Bosch, 2003). In the current air cooled alternators, one or two fans are used for

convection cooling. These fans add to the alternator (aerodynamic) losses and are also responsible for an important part of the alternator audible noise at higher speeds.

2.3.2. Copper losses

As shown in Table 1, the main losses in the alternator are the stator copper losses. Increasing the filling factor will reduce copper losses, however, this is limited by the industrial production constraints (Beretta, 2008).

Other sources of ohmic losses include the losses in the rectifier diodes, regulator losses and and losses occurring due to the contact resistance between the slip rings and brushes.

2.3.3. Magnetic losses

At nominal excitation current and at lower speeds, the output current is low and the stator is fully saturated due to the weak magnetic reaction. This will result in important magnetic losses in the stator core. Increasing the speed and output current while maintaining the same excitation reduces the flux density in the stator. With this demagnetisation effect the magnetic losses become proportional to speed itself rather than the square of speed (as expected in no-load conditions). Reducing the lamination thickness can lead to a significant reduction of the magnetic losses (0.5 mm or 0.35 mm instead of 1 mm).

Since the claw pole parts are made of solid forged iron, the eddy currents can easily circulate. This will also add to magnetic losses at very low speeds and low loads where the flux density in the air-gap (generated mainly by excitation field) is modulated by the stator slot openings. At higher speeds, the stator magneto-motive force (MMF) produces space harmonic fields in the air-gap which are augmented by the slot openings and again produce claw-pole eddy currents (Boldea, 2006). To reduce magnetic losses in the rotor, it is possible to use a laminated material but the assembly process is more complex (Bretta, 2008).

2.3.4. Cooling of the alternator

An efficient cooling method is necessary to limit the temperature in the motor beyond the permissible limits (a junction temperature of 200°C for the diodes and the stator winding).

The thermal dissipation in an alternator is mainly by convection through one or two cooling fans. The small amount of heat generated in the rotor can be dissipated by conduction through alternator bearings.

As an alternative to air cooling, it is possible to cool the alternator more efficiently with a circulation of the engine coolant in the alternator housing. It also reduces the alternator's noise level by omitting the cooling fan(s).

3. Alternator modeling for performance analysis

In order to evaluate the performance of the alternator under variable load conditions, both the machine and rectifier systems shall be modeled with appropriate magnetic and electrical models.

3.1. Electrical modeling of the Lundell alternator with an equivalent circuit

3.1.1. Electrical modeling of the machine

A 3-phase synchronous machine can be modeled by its equivalent circuit as shown in fig. 4. The parameters of the electrical alternator model are derived from the no-load EMF versus rotor field current characteristic $E_V(j_{rotor})$ and the short circuit characteristic $I_{CC}(j_{rotor})$. The stator cyclic inductance ($L(j_{rotor})$) is derived from both tests by applying Eq. 1 where ω is the electrical frequency.

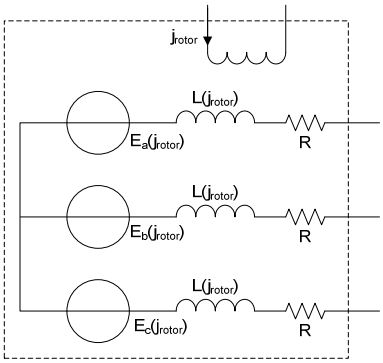

Figure 4. Equivalent circuit model of a 3-phase synchronous machine

A high rotor field current produces magnetic saturation and the stator inductance value decreases. The accuracy of such a model highly depends on the parameters identification or computation method. The armature phase resistance is measured at the rated temperature rise.

$$L(j_{rotor}) = \frac{E_V\left(j_{rotor}\right)}{\omega \cdot I_{CC}\left(j_{rotor}\right)} \tag{1}$$

3.1.2. Modeling of the alternator- rectifier

It is possible to evaluate analytically the steady state performance of a 3-phase alternator - rectifier system connected to a voltage source (fig. 5) as shown in (Figueroa et al., 2005). This type of modeling uses the electrical equivalent circuit of the machine to directly determine the steady state copper losses, current harmonic contents and DC bus current.

It is faster than a step by step simulation method as employed by simulators for power electronics (PSIM, Saber) and it is well adapted for use within an optimization loop for system evaluation purposes. However, it uses simplifications which compromise the accuracy of the results including rotor saliency, and magnetic losses in the machine.

To evaluate the simulation method, an experimental set-up is used to compare the output performance of the alternator with various rectifier topologies (fig. 6). Torque is measured by a rotating torque sensor and a strain gauge. The alternator is driven by a 5 kW DC motor

via a belt and pulley system. A position encoder is also available. The rectifier has been taken out from the machine and the voltage regulator has been removed so that the excitation current could be imposed using an external current source. The same experimental set-up will allow the comparison of various converter topologies and winding configurations for alternators. It has been used for all the experimental work presented in this chapter.

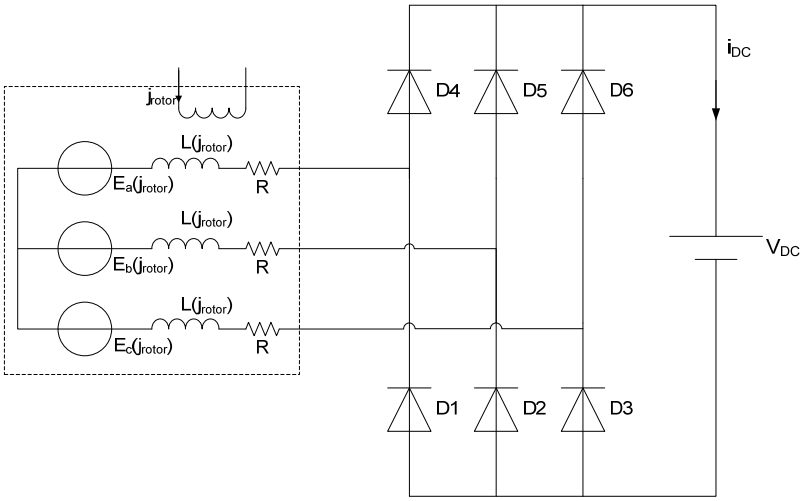

Figure 5. Circuit model of a generation system with a diode rectifier

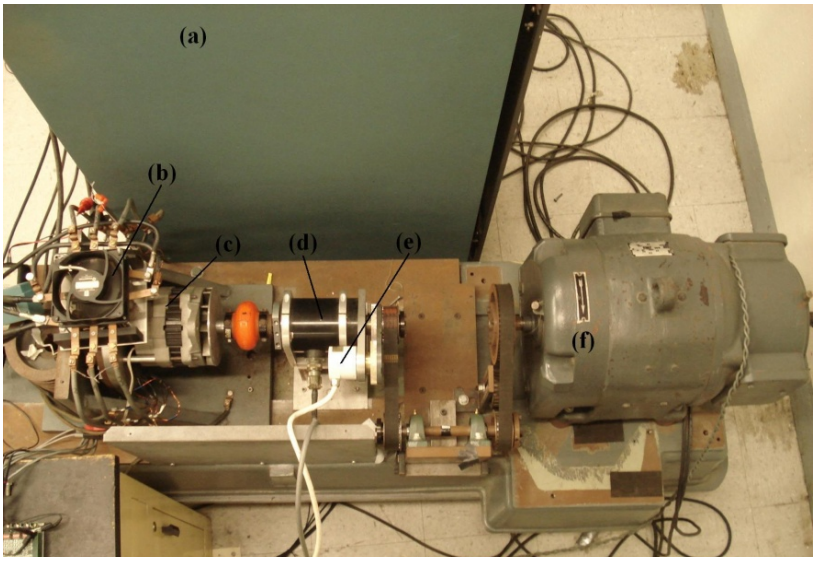

Figure 6. Test bench, a) converter (b) conventional rectifier, (c) alternator, (d) torque sensor, (e) position sensor, (f) DC motor

Fig. 7 shows the characteristics of the output maximum current and efficiency versus speed provided by the manufacturer along with those obtained by simulation. The simulation slightly overestimates the output current particularly in the central part of the curve. This could be explained by the absence of magnetic losses in the simulation, assumption of a sinusoidal EMF and inaccuracies in parameter identification. Despite these drawbacks, it can be seen that the proposed model is able to provide a current versus speed curve of satisfactory accuracy. In the same figure, it can be seen that the absence of the magnetic and mechanical losses leads to a significant overestimation of the efficiency.

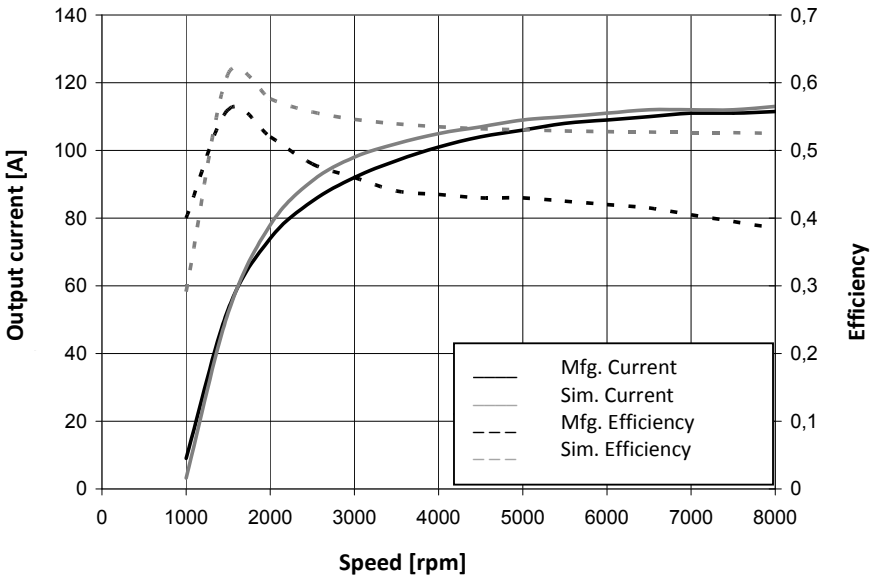

Figure 7. Comparative analysis of simulation and experimental results (from manufacturer) of the alternator output characteristics

3.2. Simulation limitations

The use of a PWM controlled rectifier (fig. 8) instead of a diode rectifier allows for the following main benefits: boosting operation for increasing the output power at low speed and power factor correction in the machine for maximization of output power.

In Lundell alternators, the magnetic circuit is saturated for the rated field current. With a Conventional Diode Rectifier (CDR), the armature reaction always has a demagnetizing effect since the voltage is in phase with the current. In case of controlled rectifiers, the armature reaction can have a magnetizing effect at low speeds depending on the power angle. Therefore, the power increase due to power angle control is less significant than what one could expect when magnetic saturation is increased by the armature reaction. As shown in fig. 7, the simplified electrical model provides a good current estimation in the case of the diode rectifier while the magnetic saturation of armature field is neglected. This is not the

case with a PWM rectifier and the output current is often over estimated by the simulation as shown in fig. 9.

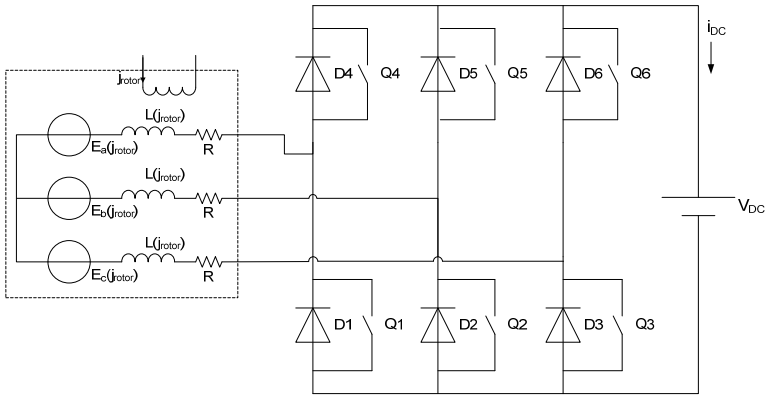

Figure 8. Circuit model of a generation system with a PWM controlled rectifier

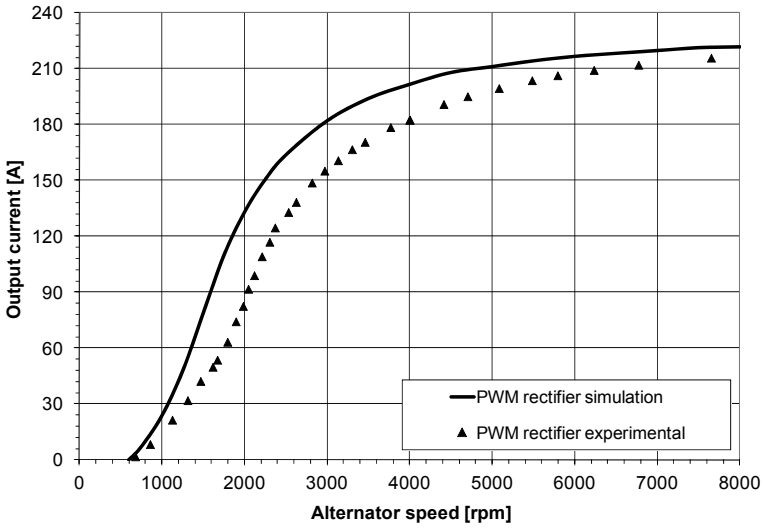

Figure 9. The output current obtained by simulation for a diode rectifier and a PWM full-bridge rectifier compared to experimental results

3.3. Magnetic modeling

Different magnetic models can be used to compute the parameters of the machine's equivalent circuit, provided that they take account of magnetic saturation.

A first one is based on a magnetic reluctance network that takes into account the machine geometry and the magnetic material B(H) characteristic (Ostovich et al., 1999). The analytical method based on the reluctance network is fast due to its simplifying assumptions.

A second method is based on 3 Dimensional Finite Element (3D FE) modeling (Küppers & Henneberger, 1997) which is particularly interesting for the analysis and evaluation of saturation and magnetic losses. Finite element methods are the most accurate but are time consuming for a variable speed machine and under variable load conditions.

Fig. 10 shows the results of 3D FE simulation of a claw pole alternator with 36 slots and 12 poles. With the 3D FE modeling, the electrical parameters of the alternator can be directly obtained by applying two methods: a method using the scalar potential and another one using the vector potential (Cros et al., 2008). Fig. 11 shows the output current versus speed characteristics obtained with the electrical parameters of scalar potential and the vector potential models. The right characteristic is between the two curves (Henneron et al., 2004).

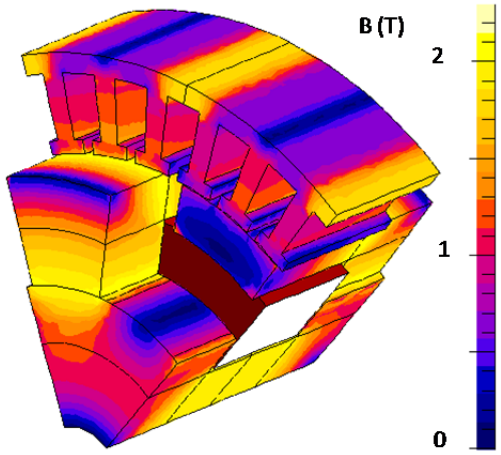

Figure 10. The results of 3D FE simulation of a claw pole alternator

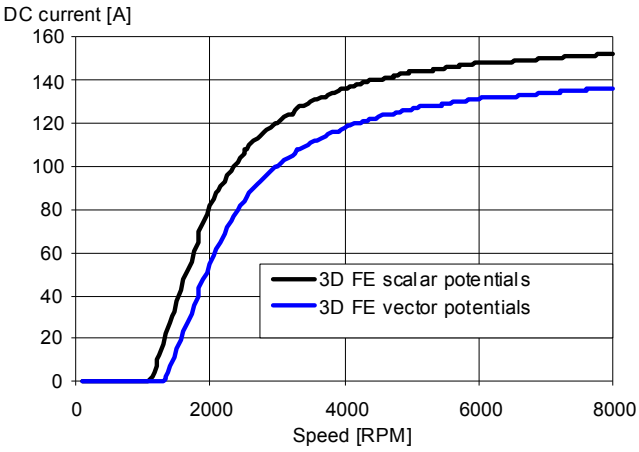

Figure 11. Simulated DC current output vs speed characteristics with two 3D FE methods

4. Improving the alternator's performance

This section focuses on various possible solutions to increase the output power of Lundell alternators without any geometry modification. This can be achieved by a winding reconfiguration to modify the number of turns per phase. A low number of turns increases power at high speed and a high number of turns improves the idle current. Another way is to rewind the alternator with a lower number of turns and to replace the conventional diode rectifier by an active PWM rectifier. The active rectifier boosts the alternator voltage in order to attain acceptable performances during low speed operation.

4.1. Influence of the number of turns on the performance

The number of turns in the stator winding has a significant effect on the output performances of an alternator connected to a Conventional Diode Rectifier (CDR) and a battery. The output current and the efficiency during high-speed operation can be easily increased by reducing the number of conductors per phase. However, the reduction of the number of turns presents also an unacceptable drawback which is a severe reduction of the output power during idle operation. On the other hand, one should increase the number of turns to improve performance at low speeds.

If the total copper cross section is not modified, the maximum current density is always the same and so the copper losses are not increased. Equation (2) shows the electrical parameters variation of the stator equivalent model (resistance R, cyclical inductance L and no-load flux Φ) according to the number of conductors per slot N when the total copper cross section is kept constant.

$$L = N^2 \cdot L_0 \quad , \quad R = N^2 \cdot R_0 \quad , \quad \phi = N \cdot \phi_0 \tag{2}$$

Fig. 12 shows a comparison of output characteristics with a number of turns per phase divided by two. The stator winding with the highest number of turns halves the speed of the generation starting point but it produces twice less output current during high-speed operation. One can notice that the winding with twice less turns provides better performance (higher current with lower copper losses) as soon as the speed exceeds 2700 rpm.

4.2. Winding reconfiguration

Winding reconfiguration is an interesting approach to improve output power, efficiency and satisfy idle current specifications.

4.2.1. Delta-wye and the series-parallel reconfiguration

One solution is to divide each phase winding in several coil groups and to modify the winding configuration by using several switches. It is then possible to obtain different connections of the coil groups (parallel, series, delta, wye) as a function of the speed. Fig. 13 shows the delta-wye and the series-parallel reconfiguration (Liang et al., 1999).

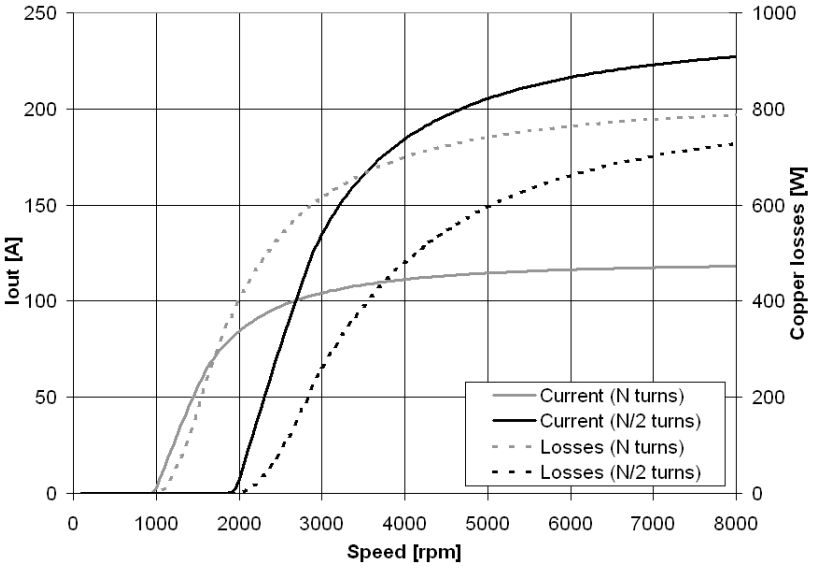

Figure 12. Influence of winding number of turns on the output performance with a diode rectifier

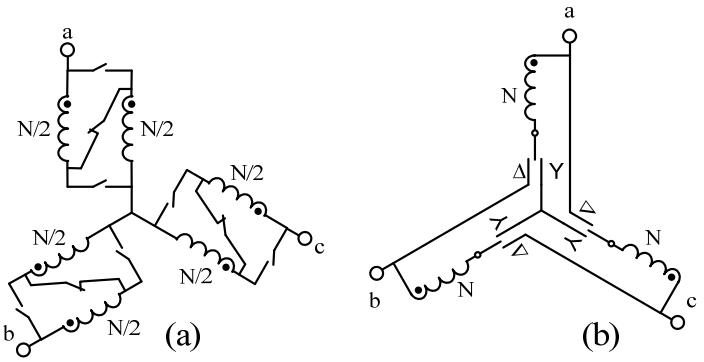

Figure 13. a) Series- Parallel reconfiguration, b) Wye- Delta winding reconfiguration

4.2.2. Multi-winding stator with series/parallel diode rectifier

One can also use a multi-winding stator with different number of turns to adapt the output characteristics (output current and efficiency) with a single voltage output. In this case, the different windings are connected to different diode rectifiers and must be magnetically decoupled (Cros et al., 2003). In order to compare the relative performance, we consider a given stator with the electrical parameters of a single-winding configuration (L_0, R_0 and Φ_0). Equation (3) shows the new electrical parameters of a m-winding configuration in the same stator.

$$L_i = N^2 \cdot \frac{L_0}{m} \quad , \quad R_i = N^2 \cdot \frac{R_0}{m} \quad , \quad \phi_i = N \cdot \frac{\phi_0}{m} \tag{3}$$

If we consider m=2, it is possible to optimize the first winding system for the lower speeds and the second one for the higher speeds by choosing the right number of turns in each winding while maintaining the same copper volume per slot. For example, one may use N conductors for the first winding and N/2 conductors for the second one, as shown in fig. 14.

Fig. 15. shows a comparison of output characteristics between a single-winding configuration with N conductors per slot and the double-winding configuration of fig. 14. Note that the double-winding configuration provides higher output current when the speed is greater than 2700 rpm but the current is reduced at low-speed.

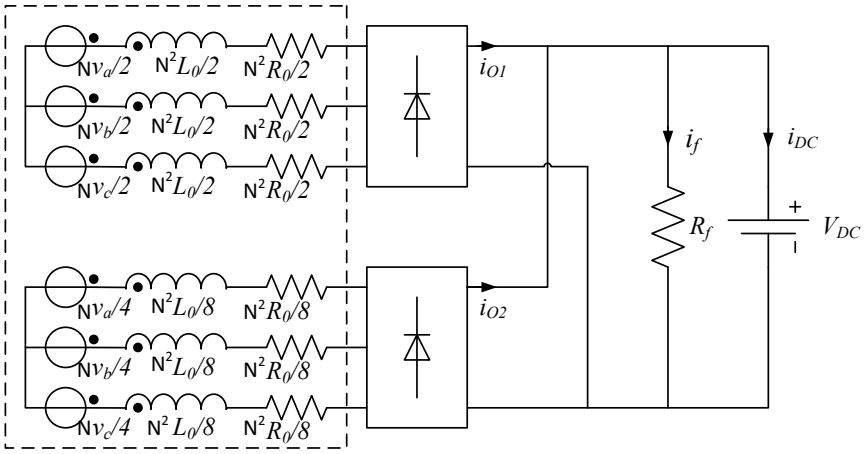

Figure 14. Multi- winding alternator with a number of turns equal to N for the first winding and N/2 for the second one.

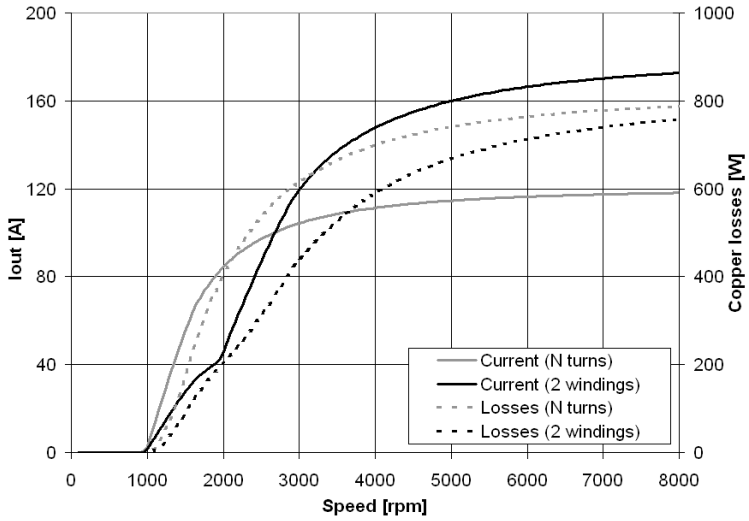

Figure 15. Performances comparison with a multi-winding stator configuration

To improve the performance over the whole speed range, it is more interesting to use the same number of turns in the two winding systems and make parallel/series reconfigurations at the rectifier outputs as shown in fig. 16. This method is easier to implement than the AC phase winding reconfiguration. It uses only one unidirectional switch and two additional diodes. Fig. 17 shows the performances of a double-winding configuration using the same number of conductors per slot as the original single-winding. A series connection provides the same output current as the original alternator, during low-speed operation when diode voltage drop is neglected. Once the speed exceeds 2700 rpm, a parallel connection is used to obtain higher output current and lower copper losses.

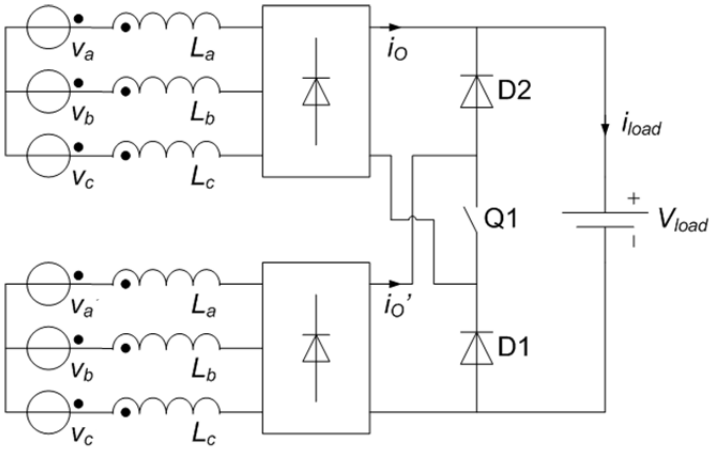

Figure 16. Reconfigurable parallel/series diode rectifiers

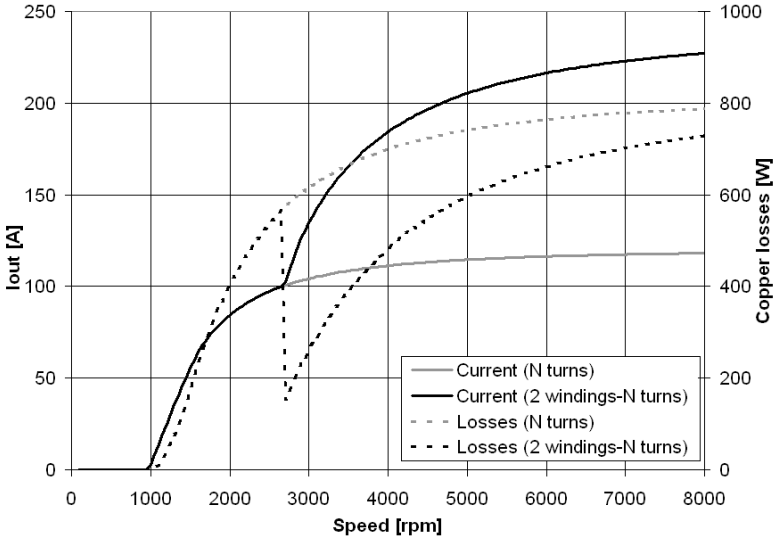

Figure 17. Performance of reconfigurable parallel/series diode rectifiers

4.2.3. Determination of parameters for rewound and multi-winding alternators

The winding scheme of a reconfigured alternator compared to the original one (Delcotron 22SI Type 12V-100A) is depicted in Fig. 18. In order to minimize the magnetic coupling, the first 3-phase winding is wound using half stator (18 slots) and the second 3-phase winding using the other half. The new lap windings have the same coil pitch as the original alternator and 12 conductors per slot. The alternator parameters are given in Table 2. The magnetic coupling between the two 3-phase winding systems has been measured for different rotor positions and the maximal measured mutual inductance between them reaches 4% of the measured self-inductance.

Assuming that magnetic coupling is negligible, the electrical parameters of a multiple three phase winding system can be computed from the original alternator parameters (L_0, R_0, Φ_{NL0} with N_0 conductors per slot). When the same stator is rewound with m three-phase windings and N conductors per slot, the new electrical parameters can be expressed as:

$$L = \frac{N^2}{m{N_0}^2} \cdot L_0 \quad , \quad R = \frac{N^2}{m{N_0}^2} \cdot R_0 \quad , \quad \phi_{NL} = \frac{N}{mN_0} \cdot \phi_{NL0} \tag{4}$$

The analysis of these equations and the experimental results (Table 2) confirms that both winding systems are magnetically decoupled.

	Original	Rewound	Double-Winding
Armature connection	Delta		
Pairs of poles	6		
Stator slots number	36		
Nominal field current	6 A		
Turns per slot	11	6	12
Wire cross section	1.75 mm²	3.30 mm²	1.65 mm²
Resistance at 25°C	0.1 Ω	0.035 Ω	0.07 Ω
Cyclic Inductance (I_f = 6A)	390 μH	115 μH	225 μH
No-load flux (I_f = 6A)	28.6 mWb	15.8 mWb	16.0 mWb
Generation-starting speed (I_f = 6A)	910 rpm	1670 rpm	1650 rpm
Output current at 8000rpm (I_f =6A)	116 A	215 A	218 A
Efficiency at 8000rpm (I_f = 6A)	38 %	53 %	53.5 %

Table 2. Alternator parameters (Delcotron 22si type 12v-100a)

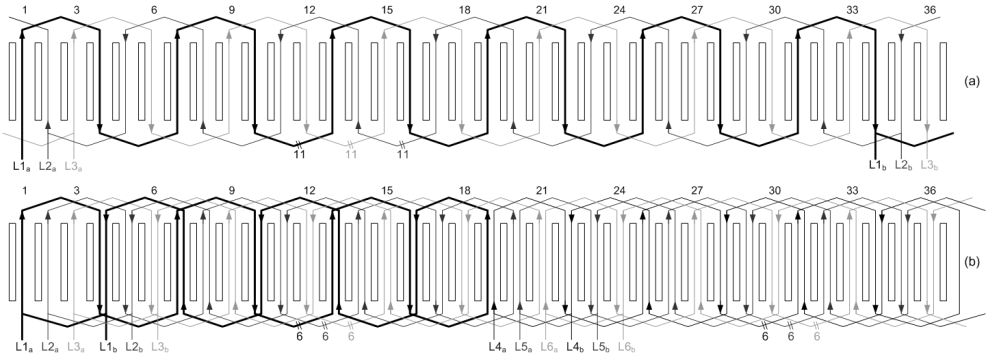

Figure 18. Winding scheme: (a) original 3-phase Delcotron alternator, (b) double-winding Delcotron alternator

4.3. Alternative converter solutions

4.3.1. Synchronous rectifier

A synchronous rectifier is an interesting alternative to conventional diode rectifiers. The main advantage of such converters is the reduced rectifier losses particularly at higher speeds if MOSFETs with low on-resistance (e.g. 4 mΩ (Beretta, 2008)) are used. Besides, it may be also employed in applications where bidirectional power transfer is required such as stop-start system (Beretta, 2008). In a start-stop system developed by Citroën, the claw-pole machine performs the functions of both starter and alternator. In the starter mode, the phase current and EMF in each phase are synchronised for maximum torque using a position sensor. In the alternator mode, the converter operates as a synchronous rectifier. The voltage drop may be as low as 0.2 V for an output current of 120 A in contrast to 0.8 V to 1.1 V for a diode. The losses can be 60 % lower compared to a diode rectifier (Beretta, 2008). In both modes of operation the switching losses will be much lower than PWM converters due to lower switching frequency. In the alternator mode the switching frequency may be as high as 2800 Hz (at 4000 rpm), however the drain currents are kept close to zero during MOSFET switching (Beretta, 2008).

4.3.2. PWM controlled full-bridge rectifier (PFBR)

In order to exploit the alternator at its maximum capabilities, it is interesting to set an optimum power angle as proposed in (Liang et al.,1999) and (Liang et al.,1996). This can be achieved with a PWM full-bridge rectifier (PFBR) as already shown in fig. 8. For each point of operation, the modulation index k and the angle θ between phase voltage and back-EMF are adjusted to maximize the output power with sinusoidal PWM control.

A PFBR is a quite expensive and complex solution; it counts for several active switches and requires rotor position sensing or complex sensorless algorithms (Boldea, 2006). However, like a synchronous rectifier, it offers bidirectional power flow control.

Fig. 19 shows the maximum output current and efficiency obtained by using a sinusoidal PWM and a control technique maximizing output power. It also shows the output current curves obtained with original and rewound alternators connected to a conventional diode rectifier. If compared to the rewound alternator with CDR (RACDR), the PFBR connected to the same alternator increases the output power for speeds below 4000 rpm. (For winding parameters see Table 1). During high speed operation, it is preferable to operate in synchronous rectification mode.

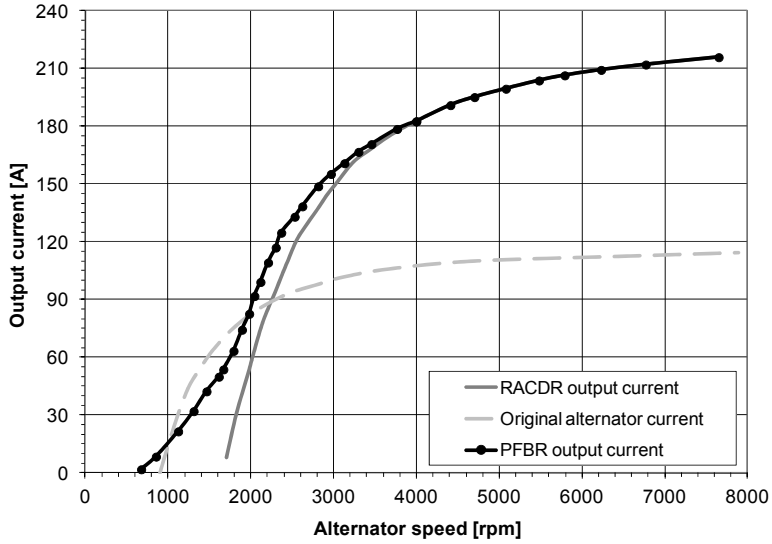

Figure 19. Experimental output current and efficiency vs. speed using a PFBR

The comparison of the output current characteristics with the original alternator shows that the current generated with the PFBR is lower in the range of 1000 to 2000 rpm (Fig. 19). Note that idle power requirement is not satisfied with the PFBR. This is partly due to the magnetic saturation and significant voltage drops across active switches.

4.3.3. Other PWM rectifiers

If bidirectional power flow is not required, the three single-phase BSBR structure shown in fig. 20 is a simpler solution. It has twice less active switches and all of them are referenced to the ground. Active switches can be reduced to only one using a Boost Switched-Mode Rectifier (BSMR), shown in fig. 21. With this topology, it is not necessary to use a rotor position sensor but the power angle can't be controlled.

4.3.4. High frequency ripple reduction of the output current using interleaving

All presented PWM rectifier topologies deliver an output DC current with abrupt current steps and high *di/dt's*. These high-amplitude fast-moving current transitions generate RF

noise that flows to the battery and then pollutes other loads connected to the battery. Attenuation of these current variations to an acceptable level requires a very large output capacitor. This can lead to considerable efforts to comply with EMC standards (Maxim, 2001). Battery current ripple results in battery heating and a corresponding rise in temperature.

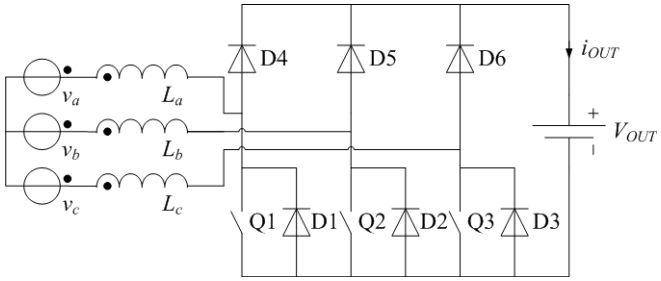

Figure 20. Boost semi-bridge rectifier (BSBR)

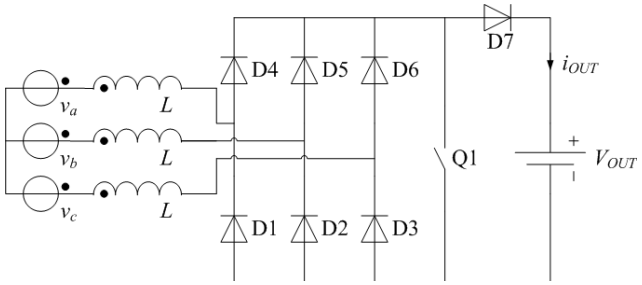

Figure 21. Boost switched-mode rectifier (BSMR)

Benefits of interleaved converters on current ripple, components stress and EMI reduction are well known for several different applications (Consoli et al., 2004), (Crebier et al., 2005). The main constraint of interleaved structures is the magnetic coupling between the different windings. Both converters must be connected to different three-phase windings that are not magnetically coupled to avoid a decrease of performances. Fig. 22 shows an example of two interleaved BSMRs with two identical three-phase winding systems having a same back-EMF. Q1 and Q2 are driven by two signals having the same duty-cycle and the same frequency but the phase is shifted by 180 degrees.

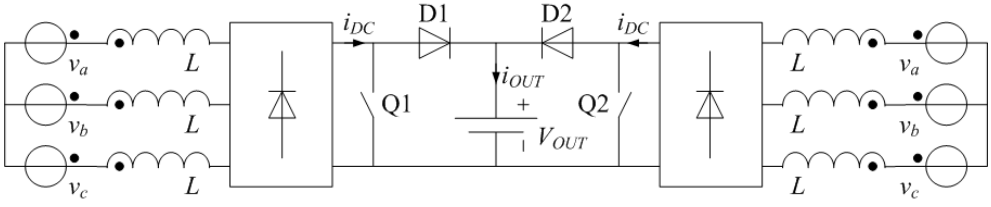

Figure 22. Two interleaved BSMRs connected to two identical three-phase windings

Interleaving decreases the current ripple for any value of duty-cycle and it allows for total ripple cancellation when D = 0.5. Equation (5) gives the optimal duty-cycle for a number m of interleaved rectifiers where k_i is an integer.

$$D_{opt} = \frac{1}{m}\left(m - k_i\right) \quad with \quad 0 < k_i < m \tag{5}$$

4.3.5. PWM BSMR with high frequency ripple cancellation

The structure of fig. 23 could be also implemented using the double-winding stator system presented above and two BSMRs operated with fixed optimal duty-cycle (D = 0.5). The rectifier control is thus extremely simple and no position sensing is required. Experimental current waveforms are shown in fig. 23 (left). When comparing the output current ripple with the one obtained with the non-interleaved converter presented in fig 23 (right), one can appreciate the considerable output current ripple reduction due to interleaving. (from 66A rms to 6.1A rms).

4.3.6. PWM BSBR with high frequency ripple cancellation

It is also interesting to operate two interleaved BSBRs with a fixed duty-cycle of 0.5 to obtain an ideal ripple cancellation. Hence the simplest control mode consists in driving all the switches of the first converter with the same gate signal and all the switches of the second converter with the same complementary signal. This method doesn't require additional rotor position sensing. Since the duty cycle is fixed at 0.5, no more control of the power angle is achievable.

The BSBR has a voltage drop per device less than the BSMR. This leads to better performance over the whole speed range

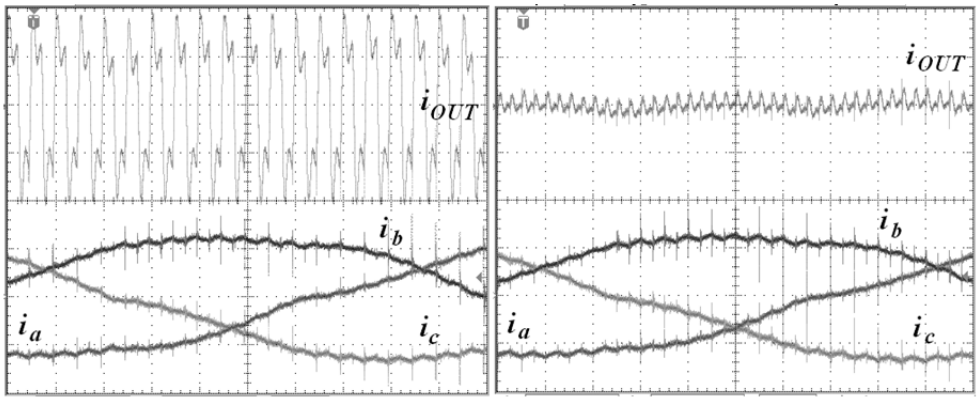

Figure 23. Experimental current waveforms for: left) interleaved BSMRs; right) non-interleaved BSMRs, at 2000rpm with If = 6A. (Vertical scale: 60 A/div, horizontal scale:200 μs/div)

4.4. General comparison

To compare the power improvement provided by the different rectifier topologies, the average power output $P_{avg.}$ and efficiency $\eta_{avg.}$ are estimated over the same drive cycle (a combination of the two vehicle speed cycles EPA UDDS and EPA US06) using the steady state performance curves with the rated field current. The results are given in Table 2.

Over the same driving cycle, the average power increase with respect to the original alternator ranges from 62% to 67% depending on the topology. The average efficiency has been improved by 10.6 to 11.5 percentage points.

The average output power and the efficiency are very similar for all the structures connected to a rewound machine since all structures regain the conventional diode rectifying mode during high-speed operation. In fact, the controlled rectifier is essentially used at idle speed.

Remarkable differences are although noticeable on the idle mode output power. Note that none of the topologies regains the original idle power. The closest idle power is obtained with the CSPR (-13%). Furthermore, the BSMR and BSBR deliver surprisingly more output power when interleaving is used. This can be partially explained by lower ESR losses in the output capacitor. However, the fact that two different machines are used (single-winding alternator and double-winding alternator) can have an influence too.

The approximate cost estimation for each solution can be derived from the number and ratings of the semiconductors and from the output filter size. It is assumed that the machine cost is not affected by rewinding and the filter size is proportional to the AC ripple component of the output current.

For semiconductors sizing, only rms current ratings are taken in account. In fact, in all topologies, each switch has to withstand the same reverse voltage which corresponds to V_{OUT} (voltage transients neglected). Current ratings are normalized with respect to I_{SC}. Table 3 shows the parts count and their ratings for each topology.

Topology	P_{idle}		$P_{avg.}$		$\eta_{avg.}$
Original Alternator	1059W	1.0pu	1454W	1.0pu	42.4%
Rewound alternator with PFBR	899W	0.85pu	2430W	1.67pu	53.6%
Rewound alternator with BSBR	831W	0.78pu	2413W	1.66pu	53.9%
Rewound alternator with BSMR	779W	0.74pu	2350W	1.62pu	53.4%
Double-winding alternator with interleaved BSBR	869W	0.82pu	2419W	1.66pu	53.8%
Double-winding alternator with interleaved BSMR	799W	0.75pu	2353W	1.62pu	53.0%
Double-winding alternator with CSPR	918W	0.87pu	2389W	1.64pu	53.5%

Table 3. Idle power, average output power and efficiency over the same driving cycle for each topology

In the case of interleaved structures, semiconductor parts are multiplied by two. However, the active silicon area remains the same and distribution of switching power can eventually even be advantageous. Also note that for non-interleaved structures using PWM, the rms value of the ripple component of the output current is about 10 times more significant than

with other structures. The resulting filtering requirements for EMC standards compliance can easily lead to bulky and expensive solutions.

Topology	Number of Slow diodes	Slow diode rms current (I_{SD})	Number of Fast diodes	Fast diode rms current (I_{FD})	Number of Active switches	Active switch rms current (I_Q)	Output current AC ripple (I_{AC})
Original Alternator	6	0.52pu	-	-	-	-	0.04pu
PFBR	-	-	6	0.52pu	6	0.37pu	0.48pu
BSBR	3	0.52pu	3	0.52pu	3	0.37pu	0.5pu
BSMR	6	0.52pu	1	1.0pu	1	1.0pu	0.5pu
Interleaved BSBR	6	0.26pu	6	0.26pu	6	0.18pu	0.04*pu
Interleaved BSMR	12	0.26pu	2	0.5pu	2	0.35pu	0.04*pu
CSPR	12	0.26pu	2	0.5pu	1	0.5pu	0.04pu

* neglecting HF ripple through inductances

Table 4. Semiconductor parts count and normalized current ratings for each topology

5. Conclusion

The low efficiency and the limitation of the output power are major drawbacks of the Lundell alternator. Replacing these alternators with other types of machine is not an economic choice because of their low manufacturing cost. However, improving the performance of existing machines is still the best way for the short term future. This chapter discusses the performance of the conventional automotive alternators and various modeling methods for the simulation of the alternator-rectifiers. Some improvements without geometry modification have been proposed and validated using standard frame of automotive alternator. The results show that the modification of the number of turns and replacing the diode rectifier with other electronic converters could significantly increase the output current and the efficiency. However, there are many other possibilities for enhancing the performance which have not been considered. For example, the transition from 14V to a 42V system, will allow to increase the efficiency of the power electronics rectifier by reducing the conduction losses. The optimization of the claw-pole machine, the use of hybrid structure with permanent magnets, laminations of higher quality, and liquid cooling are alternative methods to enhance the performance.

Author details

Ruben Ivankovic, Jérôme Cros, Mehdi Taghizadeh Kakhki,
Carlos A. Martins and Philippe Viarouge
Laval University, Canada

6. References

Beretta, J. (2008). *Electronique, électricite et mecatronique automobile*, Lavoisier, ISBN:978-2-7462-1245-9, Paris

Boldea, I. (2006). Automotive Claw-Pole-Rotor Generator Systems, In: *Variable speed generators*, Taylor & Francis Group, ISBN 0-8493-5715-2

Bosch (2003). Alternators, In: *Automotive electrics and electronics*, Bauer, H., pp. 112-163, SAE International, ISBN 0-7680-0508-6, Stuttgart

Consoli, A.; Cacciato, M.; Scarcely, G. & Testa, A. (2004). Compact, reliable efficiency. *Industry Applications Magazine, IEEE*, vol.10, no.6, pp. 35- 42, Nov.-Dec. 2004

Crebier J.C.; Revol, B. & Ferrieux J.P. (2005). Boost chopper derived PFC rectifier: Interest and Reality. *IEEE Transactions on Industrial Electronics*, Vol.52, No.1, February 2005, pp 36-45

Cros, J.; Paynot, C.; Figuerora, J. & Viarouge, P. (2003). Multi-Star PM brushless DC motor for traction application, *EPE'2003*, Toulouse, 2-4 sept. 2003.

Cros, J; Radaorozandry, L; Figueroa, J & Viarouge, P. (2008). Influence of the magnetic model accuracy on the optimal design of a car alternator, in *Int. Journal for Computation and Mathematics in Electrical and Electronic Engineering -COMPEL*, Vol 27, Issue 1, pp. 196-204, 2008.

Figueroa, J.; Cros, J. & Viarouge, P. (2005). Analytical model of a 3-phase rectifier for the design of a car alternator, *Proceedings of Electrimacs conference*, Tunisia, Apr. 2005

Henneron T., Clénet S., Cros J. & Viarouge P. (2004), "Evaluation of 3D Finite Element Method to Study and Design a Soft Magnetic Composite Machine", *Magnetics, IEEE Transactions on,* Vol.40 , No2, pp786 – 789.

Kuppers, S.; Henneberger, G. (1997), "Numerical procedures for the calculation and design of automotive alternators," *Magnetics, IEEE Transactions on*, vol.33, no.2, pp.2022-2025, Mar 1997

Liang, F.; Miller, J.M. & Xu, X. (1999). A vehicle electric power generation system with improved output power and efficiency. *Industry Applications, IEEE Transactions on*, vol.35, no.6, pp.1341-1346, Nov/Dec 1999

Liang, F.; Miller, J.M. & Zarei, S. (1996). A control scheme to maximize output power of a synchronous alternator in a vehicle power generation system, in *Conf. Rec. IEEE-IAS Annual Meeting*, Oct. 1996, pp. 830-835

Maxim/ Dallas semiconductors (2001), Circuit tradeoffs minimize noise in battery-input power supplies, In: *Application note 653*, 8 pages, 22 January. 2001. Available from: http://www.maxim-ic.com/an653

Nipp, E. & Norberg, E. (1998) , "On the feasibility of switched stator windings in permanent magnet motors for traction drives," *Railroad Conference, 1998. Proceedings of the 1998 ASME/IEEE Joint* , vol., no., pp.33-39, 15-16 Apr 1998

Ostovic, V.; Miller, J.M.; Garg, V.K.; Schultz, R.D. & Swales, S.H. (1999), "A magnetic-equivalent-circuit-based performance computation of a Lundell alternator," *Industry Applications, IEEE Transactions on* , vol.35, no.4, pp.825-830, Jul/Aug 1999

Perrault, D. & Caliskan, V. (2004). Automotive Power Generation and Control. *IEEE Transactions on Power Electronics*, Vol. 19 No. 3, May 2004, pp 618-630.